

Experimental Rotor Unbalance Response Using Hydrodynamic Gas Lubrication

R. D. DAYTON

Associate Engineer, Midwest
Research Institute.

M. R. CHASMAN

Lubrication Branch, Air Force Aero
Propulsion Laboratory.

Wright-Patterson Air Force
Base, Ohio

This paper investigates the adequacy of the theoretical model in predicting the unbalance response of a rotor supported in hydrodynamic gas lubricated journal bearings. The magnitude of experimental whirl amplitudes induced by applying various unbalances to a rotor supported in hydrodynamic journal bearings were measured and compared to the theoretical predictions. Variables investigated were rotor unbalance, rotor speed, and bearing load. Reasonable agreement between the experimental and theoretical results was obtained.

Introduction

Gas lubricated bearings seem attractive for application in systems which must operate at high temperatures and high rotor speed with minimum support requirements such as lubricant feed lines and reservoirs and precise positioning of rotating elements. These systems include power generation and propulsion systems for future high speed aircraft, as well as rotating equipment for space power and machine tool applications. As a result, the technical journals which deal with lubrication technology have been saturated with papers on gas bearings during the past decade. Most of the work discussed in these

papers was performed to provide the capability to accurately predict the behavior of gas lubricated bearings through rigorous theoretical techniques. The application of the theoretical results to the design of machines requires that the theoretical information be reduced to a form which can be used by a design engineer with some confidence. The designer requires design charts, maps, and tables. Computer programs which offer the ability to obtain solutions to the applicable equations in a short time with minimum expense are also useful to the designer. References [1] and [5]¹ include design information and computer programs which were intended as tools which a design engineer can use to produce good rotor-bearing systems.

A program was initiated by the Aero Propulsion Laboratory in 1969 to evaluate the usefulness of the design information available in references [1] and [5] as applied to rigid rotor systems. The approach was to design representative bearing-rotor systems using the design information and to perform an experimental study to produce data which could be compared to the predicted (theoretical) results. The design information used may not

Contributed by the Lubrication Division of THE AMERICAN SOCIETY OF MECHANICAL ENGINEERS and presented at the ASLE-ASME Joint Lubrication Conference, Pittsburgh, Pa., October 5-7, 1971. Manuscript received by the Lubrication Division, March 22, 1971. Paper No. 71-Lub-10.

¹ Numbers in brackets designate References at end of paper.

Nomenclature

| | | |
|---|---|--|
| A = cross-sectional area of rotor, in. ² | I_p = polar mass moment of inertia of a rotor mass, lb-in-sec ² | R = rotor journal radius, in. |
| a = rotor mass eccentricity, in. | I_T = transverse mass moment of inertia of a rotor mass, lb-in-sec ² | V = shear force, lb |
| C = radial clearance, in. | K_{xx}, K_{yy} = bearing spring coefficients for translatory whirl, lb/in | x = amplitude in vertical direction, in. |
| C_{xz}, C_{xy} = bearing damping coefficients for translatory whirl, lb-sec/in. | K_{yz}, K_{yx} = bearing spring coefficients for conical whirl, lb/in | y = amplitude in horizontal direction, in. |
| D_{xz}, D_{xy} = bearing damping coefficients for conical whirl, lb-in-sec/rad | M = bending moment, lb-in. | z = coordinate along rotor length, in. |
| E = Young's modulus, lb/in. ² | M_{xx}, M_{yy} = bearing spring coefficients for conical whirl, lb-in/rad | ρ = mass density, lb-sec ² /in. ⁴ |
| I = cross-sectional moment of inertia, in. ⁴ | | ω = angular speed of rotor, rad/sec |

have been the most accurate available but was considered to be representative of the quality available to most designers. The work discussed in this paper is the portion of the experimental program which dealt with the unbalance response of a plain cylindrical gas lubricated bearing-rotor system.

Test Apparatus

The Air Force Aero Propulsion Laboratory gas bearing facility used in conducting the rotor unbalance response study was developed for the Air Force by Southwest Research Institute and consists of a bearing head assembly, test bearings and rotor, rotor drive system, test rotor displacement-measuring system, a loading system and the necessary instrumentation and controls. A photograph of the test facility is shown in Fig. 1.

Bearing Head Assembly. The bearing head assembly is housed in a stainless steel two-piece bearing housing, the two halves of which are accurately aligned by a pilot surface. The two test bearings, having tapered outer surfaces, are secured in matching tapered holes in the housing by bearing retainers. Two rotor displacement sensing capacitance probes are mounted in the bearing retainers at each end of the test rotor. Both probes are positioned perpendicular to the rotor axis and to each other. A flexible drive shaft (quill), connecting the drive motor to the test rotor, restrains the axial displacement of the test rotor. In the event the flexible drive shaft fails, carbon buffers prevent the test rotor from contacting the housing.

Test Bearings and Rotor. One set of plain cylindrical, self-acting journal bearings fabricated from SAE A-2 tool steel were used to conduct the rotor unbalance response tests. The bearings were 1.100 in. long and had a nominal inside diameter of 1.00141

in. Out-of-roundness of both bearings was less than $25 \mu\text{-in.}$ The test rotor, designated Rotor C, was 7 in. in length, weighed 5.951 lb, and had a nominal journal diameter of 1.00026 in. This resulted in a diametral clearance between rotor and bearings of 0.00115 in. and a $\frac{C}{R}$ ratio of 0.00115. Out-of-roundness and taper over the journal portions of the rotor was less than 0.0001 in. Fig. 2 shows a photograph of the test bearings and rotor.

Four threaded holes, two of which can be seen in Fig. 2, were located on the rotor circumference and were used to accommodate the various unbalances which were used in the study. The unbalances, which were made from $\frac{1}{4}$ -28 threaded rod, were positioned so as to affect each of the two test bearings equally. A photograph showing the relative size of the unbalance weights is presented in Fig. 3. Prior to testing, the test rotor was dy-

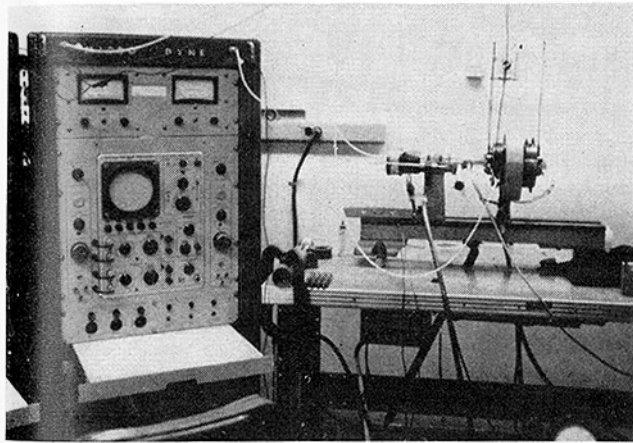


Fig. 1 Photograph of gas bearing test facility

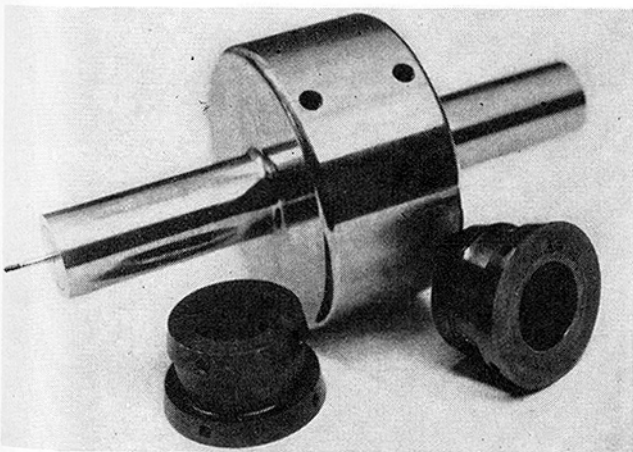


Fig. 2 Photograph of test bearings and rotor

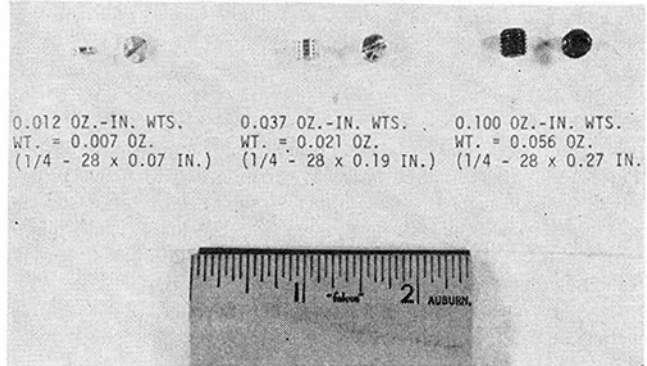


Fig. 3 Photograph of unbalance weights

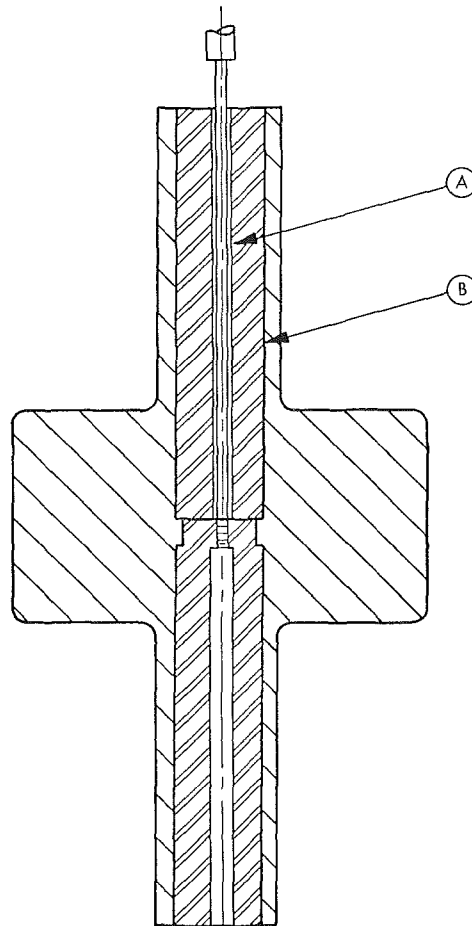


Fig. 4 Cross section of test rotor showing flexible drive shaft connection

namically balanced at a speed of 2000 rpm to approximately 0.0025 oz-in. Runs were made at this unbalance condition, referred to as no mechanically induced unbalance, to establish baseline data.

Test Rotor Drive System. The test rotor was driven by a two-phase, $\frac{3}{4}$ HP, high-speed electric motor through a flexible drive shaft. The maximum free-running speed of the drive motor was approximately 71,000 rpm. Driving rotors the size of the test rotor, the maximum speed obtainable was approximately 45,000 rpm. The flexible drive shaft was connected to the test rotor by means of screw threads located at the center of the rotor length as shown in Fig. 4. As can be seen in Fig. 4, the deflection of the flexible drive shaft in case of whipping is limited by the size of the hole (0.113 in.), A, in the metal insert, B, which surrounds the portion of the flexible shaft inside the test rotor.

Test Rotor Displacement-Measuring System. Four noncontacting capacitance probes, which had a 0- to 10-mil range capability, were used to detect the displacement of the test rotor within the bearings. The output of the four probes was input into a console analyzer which included an amplifier and detector circuit for each probe yielding a linear voltage output proportional to the displacement between the probe and rotor, a filter for each probe, and a cathode ray oscilloscope for each pair of probes. The rotor motion in each bearing was monitored by two probes which were positioned 90 deg apart. One probe represented the x -plane of the rotor-bearing system and the other the y -plane. Either two waveforms or an x - y plot of the shaft motion in the reference plane could be displayed on the oscilloscope.

Loading System. The drive motor and bearing head assembly were mounted on a modified lathe bed which could be pivoted about one end such that the test rotor axis could be rotated from a horizontal position to a vertical position. This was done by means of a screw-jack mechanism.

The radial load supported by the two test bearings was the gravitational component of the test rotor weight. The maximum load on each bearing was one-half the test rotor weight when the bearing rig was in the horizontal position, and the minimum load was essentially zero when the rig was in the vertical position. At any angle between these two extremes, the bearing load could be determined from the known weight of the test rotor and the angle of elevation of the test rig.

Experimental Approach

The experimental approach or procedure used to determine the unbalance response of the test rotor was as follows:

- 1 Calibrate the rotor displacement-measuring system,
- 2 Apply unbalance to test rotor,
- 3 Assemble and align test bearings in bearing head,
- 4 Measure assembled rotor-bearing clearances,
- 5 Mount assembled bearing head with test rotor on lathe bed and align drive motor to test rotor,
- 6 Position capacitance probes on test rig, and
- 7 Measure rotor unbalance response by determining rotor whirl amplitude and whirl frequency up to instability speeds.

The rotor displacement-measuring system was calibrated to yield a linear voltage output proportional to the displacement between the capacitance probe and the test rotor. The capacitance probes were calibrated by means of a special micrometer to give a voltage reading for a particular distance between the probe and rotor. Thus, a voltage versus distance curve could be plotted for each probe. These curves were used to convert the voltage readings into displacement readings.

Prior to assembling the test bearings in the bearing head, the appropriate unbalance was applied to the test rotor by inserting two previously weighed plugs into the two threaded holes on the same side of the rotor circumference. Each plug, which was

located flush to the rotor circumference, represented one-half of the total unbalance. With the unbalance positioned in this manner, each test bearing was affected equally. By knowing the weight of the plugs and their radial distance from the rotor axis, the magnitude of unbalance could be determined by multiplying the radial distance by the weight of the plugs.

Next, the test bearings were positioned and aligned in the bearing housing. The alignment of the test bearings was checked by using a dummy shaft which was approximately 0.0001 to 0.0002 in. smaller than the bearing diameters. This shaft was installed in the bearings and the bearing retainer blocks tightened or loosened until the shaft could be freely rotated. With this method of alignment, clearances greater than 90 percent of full clearance were obtained.

The test rotor was installed in the test bearings and clearances in the x - y planes for both bearings were measured using the calibrated capacitance probes. Rotor displacement measurements were made in two planes and clearances determined. These clearances compared very closely with previously measured bearing bores and rotor diameter measurements. Subsequent to measuring assembled rotor-bearing clearances, the assembled bearing head with test rotor was mounted on the modified lathe bed, and aligned to the test rotor drive motor. Drive motor adjusting screws were used for this alignment. Next, the capacitance probes were positioned on the test rig. The distance the probes were positioned from the test rotor was such that only the center portion of the probe calibration curve was used.

The rotor unbalance response was determined by measuring rotor whirl amplitude and whirl frequency up to the threshold of instability speed or to the point where bearing contact prevented further operation. These measurements were obtained at bearing loads of 1.488 lb and 2.976 lb per bearing and for the following four unbalances: 0.012 oz-in., 0.025 oz-in., 0.037 oz-in., and 0.050 oz-in.

The rotor speed, whirl amplitude, and whirl frequency data were measured according to the following procedure. The rotor speed was determined by a magnetic proximity pickup and an electronic rpm counter. Whirl amplitude was measured on the two oscilloscopes by noting the size of the x - y whirl orbit plot observed on the calibrated scope screen. Rotor whirl frequency was determined by switching the oscilloscope from an x - y plot to a common time base to obtain a time history of the probe output. By measuring the number of cycles obtained over a certain

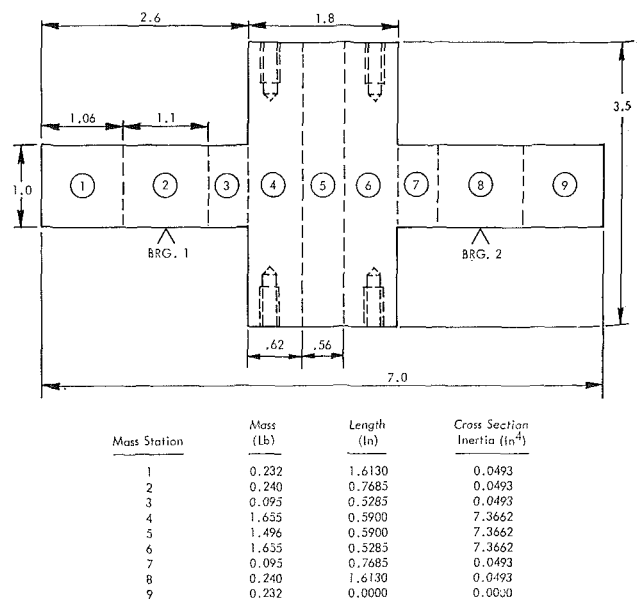


Fig. 5 Model and data for rotor C used in unbalance response program

distance of the oscilloscope trace and knowing the time base of the oscilloscope, the whirl frequency could be calculated.

Analytical Approach

The theoretical predictions compared to experimental results in this paper were obtained from a theoretical analysis which was presented in computer program form [1]. This program was capable of calculating the vibrational response of a rotor-bearing system due to a specified rotor unbalance.

The rotor dynamics analysis used in the theory was an extension of the Myklestad-Prohl method [2, 3, and 4]. The rotor model assumed was flexible and could have any arbitrary geometry. For calculation purposes the rotor was replaced by a finite number of lumped masses connected by weightless springs. The actual model and rotor data input in the computer program for Rotor C is shown in Fig. 5.

Given a rotor geometry the three basic equations used in the theory for determining rotor motion were:

- 1 Force balance for a shaft increment, dz : $\frac{dV}{dz} = \rho A \omega^2 (x + a)$
- 2 Moment balance for a shaft increment, dz : $\frac{dM}{dz} = V + \omega^2 (i_p - i_T) \frac{dx}{dz}$
- 3 Shaft deflection: $M = EI \frac{d^2x}{dz^2}$

These three equations were combined to give a differential equation governing the unbalance vibrations of a rotor:

$$4 \frac{d^2}{dz^2} \left(EI \frac{d^2x}{dz^2} \right) - \rho A \omega^2 (x + a) + \omega^2 \frac{d}{dz} \left[(i_p - i_T) \right] \frac{dx}{dz}$$

and the same for the y -direction.

At the bearings, there is an abrupt change in the shear force and the bending moment due to the bearing reactions. The change in these quantities, assuming the bearing to be at $z = z_0$, are given by the following equations:

$$5 V_{z-z_0}^+ - V_{z-z_0}^- = -(K_{xx} + i\omega C_{xx})x - (K_{xy} + i\omega C_{xy})y$$

$$6 M_{z-z_0}^+ - M_{z-z_0}^- = (M_{xx} + i\omega D_{xx})x + (M_{xy} + i\omega D_{xy})y$$

where K_{xx} , C_{xx} , M_{xx} , D_{xx} , etc., are the bearing spring and damping coefficients. These six equations provided the theoretical basis for calculating the vibrational response of the rotor-bearing system.

The dynamic bearing film properties used in the computer program for calculating the bearing reactions were represented as four spring coefficients and four damping coefficients. These coefficients contained both direct-coupling (K_{xx} , K_{yy} , C_{xx} , C_{yy}) and cross-coupling (K_{xy} , K_{yx} , C_{xy} , C_{yx}) terms, i.e., the dynamic force in a given direction was not only proportional to the amplitude and velocity components in that direction but was also proportional to the amplitude and velocity components in the mutually perpendicular direction. The values of coefficients used in making the calculations for this paper were obtained from the literature [5] and were dependent upon the particular bearing type, bearing dimensions, lubricant viscosity, bearing load, and rotor speed.

Since the bearing film properties were not the same in all directions, the whirl motion of the rotor in the analysis was treated as two dimensional such that it became an orbit around an equilibrium position. The whirl orbit was assumed to be elliptical in shape and its amplitude small when compared to bearing clearance. The computer program had the capability of calculating whirl orbits for a number of points along the rotor.

Experimental Test Results and Comparison to Theory

The rotor unbalance tests using hydrodynamic bearings were conducted at room temperature (approximately 75 deg). Results of these tests along with theoretical comparisons are presented in Figs. 6 through 19. These figures compare experimental and theoretical rotor whirl amplitudes versus rotor speed for each of the four mechanically induced rotor unbalances and the one case of no mechanically induced unbalance. Two bearing loads of 1.488 lb and 2.976 lb per bearing were investigated at each unbalance condition. Experimental data are given for each of the two test bearings and represent the maximum value of whirl amplitude obtained. Only one set of theoretical data representing both bearings is presented because of the symmetrical geometry of the rotor-bearing system. The residual rotor unbalance was assumed to be located in such a way as to affect each bearing equally, i.e., it was assumed to be located at mass station 5 and in the same plane as the mechanically applied unbalances. For the first two unbalance conditions presented in these figures, no applied unbalance and 0.012 oz-in unbalance, the experimental rotor whirl amplitudes within the free-end bearing were generally larger than those within the quill-end bearing. This is believed due to the restraints imposed by the drive quill. For the larger unbalance conditions the unbalance forces were apparently large enough to overcome the quill restraints so that the whirl amplitudes for both bearings were very nearly the same. For all unbalance and bearing load conditions, data are presented either up to the threshold of instability speed or to the point where rotor-bearing contact prevented further operation.

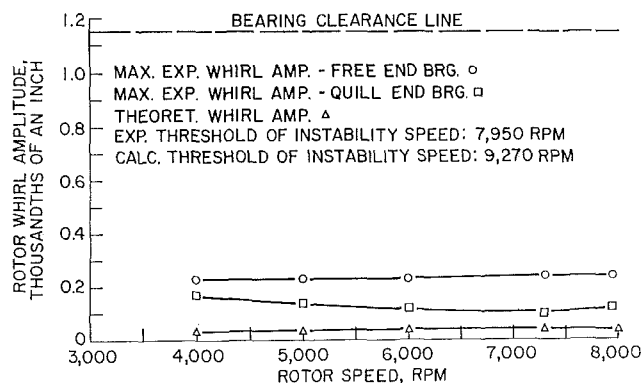


Fig. 6 Comparison of theoretical and experimental values of rotor whirl amplitude versus rotor speed at a bearing load of 1.488 lb and no mechanically induced rotor unbalance

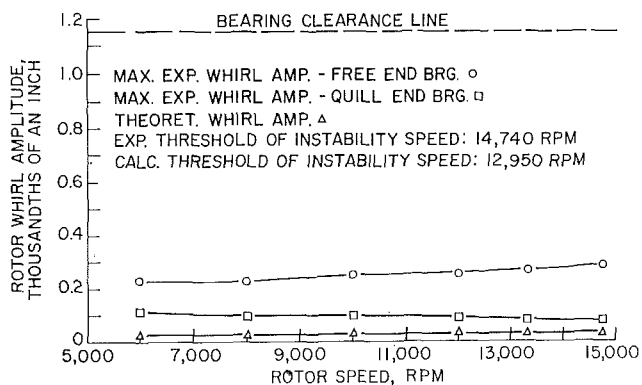


Fig. 7 Comparison of theoretical and experimental values of rotor whirl amplitude versus rotor speed at a bearing load of 2.976 lb and no mechanically induced rotor unbalance

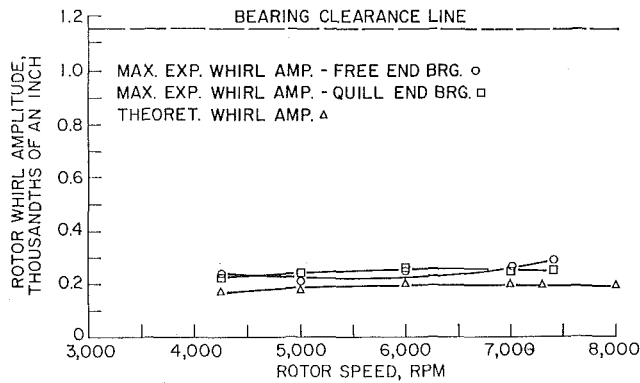


Fig. 8 Comparison of theoretical and experimental values of rotor whirl amplitude versus rotor speed at a bearing load of 1.488 lb and 0.012 oz-in. of mechanically induced rotor unbalance

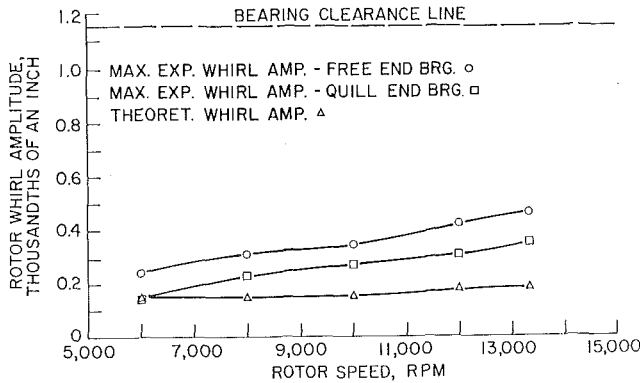


Fig. 9 Comparison of theoretical and experimental values of rotor whirl amplitude versus rotor speed at a bearing load of 2.976 lb and 0.012 oz-in. of mechanically induced rotor unbalance

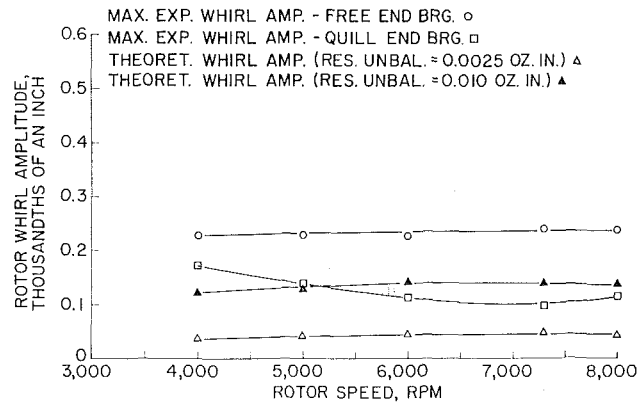


Fig. 10 Comparison of theoretical and experimental values of rotor whirl amplitude versus rotor speed at a bearing load of 1.488 lb and at various values of residual unbalance (applied unbalance: none)

Figs. 6 through 9 present experimental and theoretical comparisons for no mechanically induced rotor unbalance and 0.012 oz-in unbalance at the two bearing load conditions. For these conditions, it can be seen that the experimental values of whirl amplitude were, for all cases, larger than the theoretical values. Difference between the experimental and theoretical amplitudes for both of these unbalance conditions ranged from zero to approximately 0.00025 in., which is less than 25 percent of the total bearing clearance. Part of this difference can possibly be attributed to the difficulty of reading exact values of bearing spring and damping coefficients off of theoretical design curves [5] and

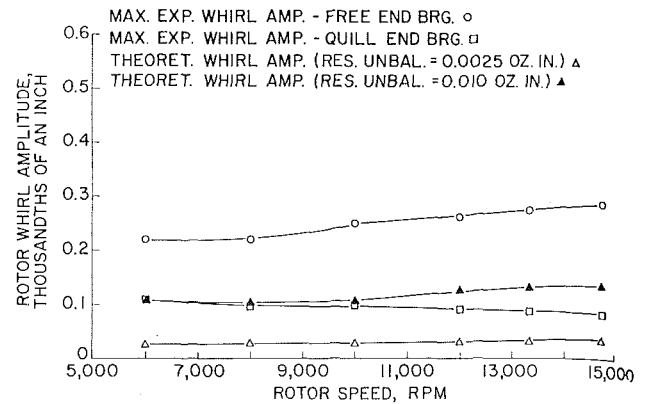


Fig. 11 Comparison of theoretical and experimental values of rotor whirl amplitude versus rotor speed at a bearing load of 2.976 lb and at various values of residual unbalance (applied unbalance: none)

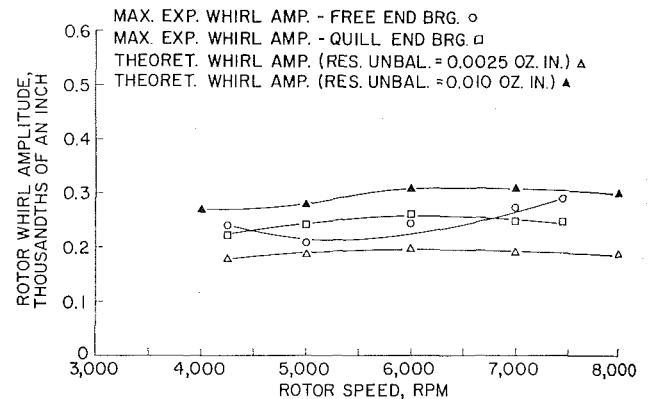


Fig. 12 Comparison of theoretical and experimental values of rotor whirl amplitude versus rotor speed at a bearing load of 1.488 lb and at various values of residual unbalance (applied unbalance: 0.012 oz-in.)

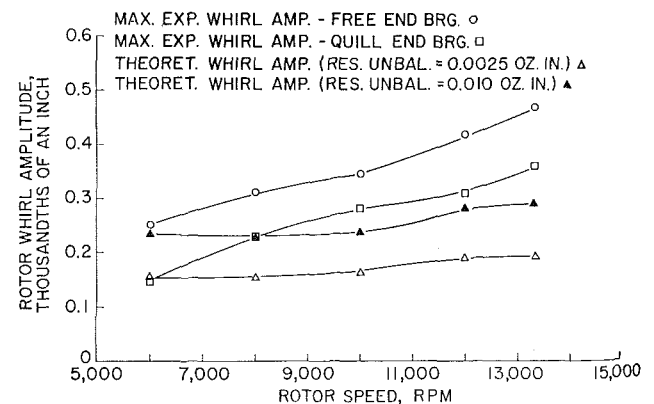


Fig. 13 Comparison of theoretical and experimental values of rotor whirl amplitude versus rotor speed at a bearing load of 2.976 lb and at various values of residual unbalance (applied unbalance: 0.012 oz-in.)

the interpolations from curve to curve which were necessary due to the variation of actual eccentricity and L/D ratios from the values used in making the theoretical design curves. The differences caused by these difficulties can, however, be considered small; i.e., they were probably less than 5 percent from the true values.

Another possibility for the difference in Figs. 6 through 9 is that the residual dynamic unbalance of the test rotor (Rotor C) as determined on a balancing machine may have been in slight error. According to the manual, this particular machine is capable of detecting displacements of 0.000025 in. corresponding

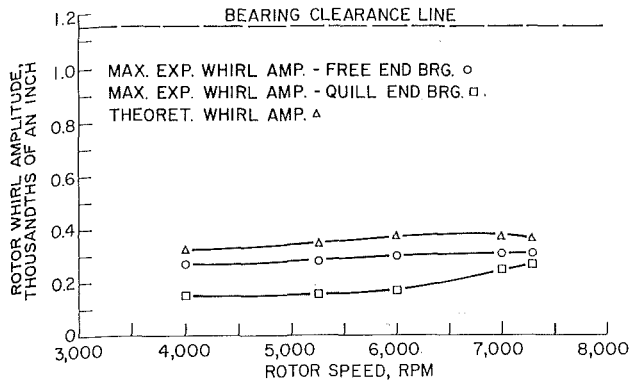


Fig. 14 Comparison of theoretical and experimental values of rotor whirl amplitude versus rotor speed at a bearing load of 1.488 lb and 0.025 oz-in. of mechanically induced rotor unbalance

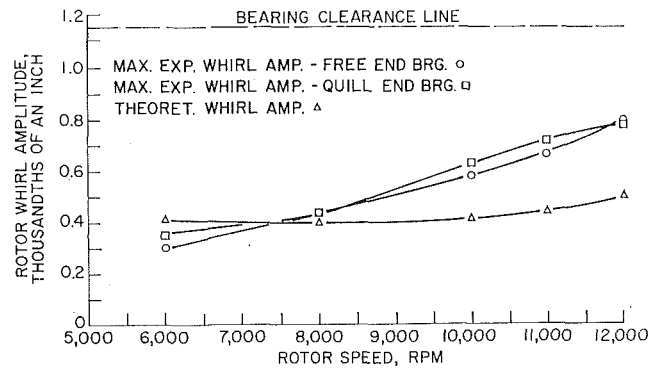


Fig. 17 Comparison of theoretical and experimental values of rotor whirl amplitude versus rotor speed at a bearing load of 2.976 lb and 0.037 oz-in. of mechanically induced rotor unbalance

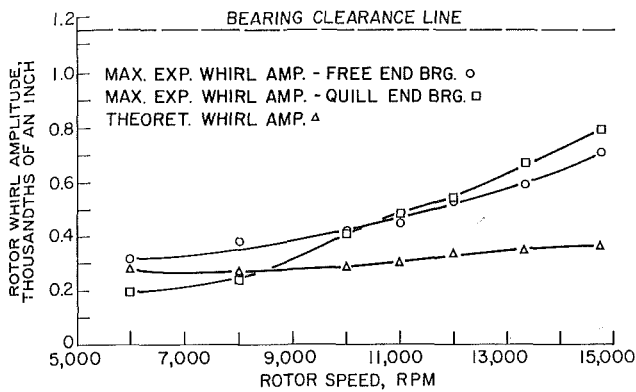


Fig. 15 Comparison of theoretical and experimental values of rotor whirl amplitude versus rotor speed at a bearing load of 2.976 lb and 0.025 oz-in. of mechanically induced rotor unbalance

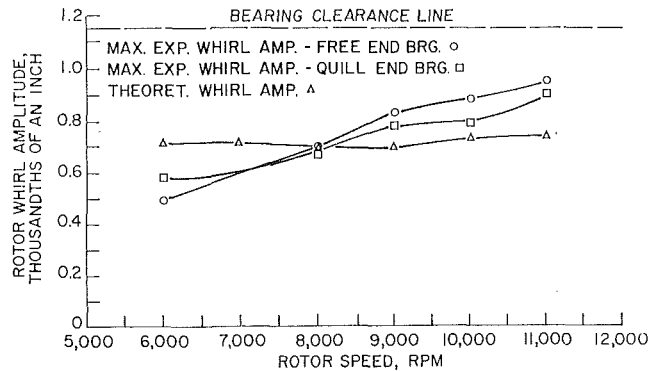


Fig. 18 Comparison of theoretical and experimental values of rotor whirl amplitude versus rotor speed at a bearing load of 1.488 lb and 0.050 oz-in. of mechanically induced rotor unbalance

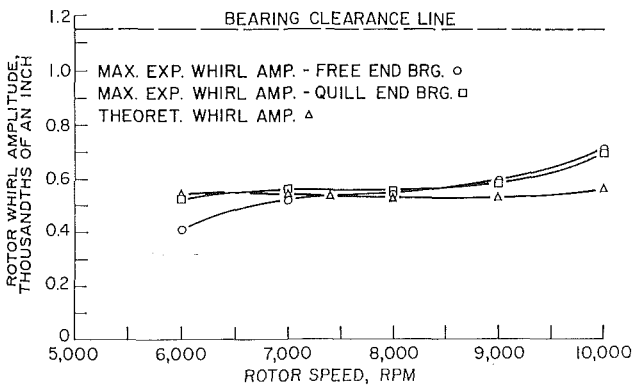


Fig. 16 Comparison of theoretical and experimental values of rotor whirl amplitude versus rotor speed at a bearing load of 1.488 lb and 0.037 oz-in. of mechanically induced rotor unbalance

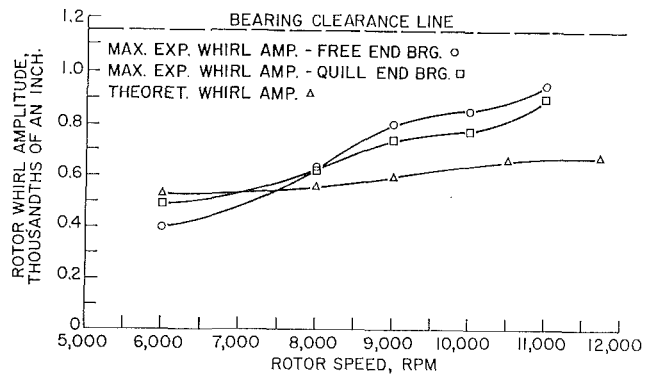


Fig. 19 Comparison of theoretical and experimental values of rotor whirl amplitude versus rotor speed at a bearing load of 2.976 lb and 0.050 oz-in. of mechanically induced rotor unbalance

to a maximum residual unbalance for Rotor C of approximately 0.0025 oz-in. This value of unbalance was the assumed value used in the computer program for all cases corresponding to no mechanically induced unbalance. If the balancing machine were slightly out of calibration, small errors in this assumed residual unbalance would result. Since whirl amplitudes are directly related to the amount of rotor unbalance, any difference in the true and assumed values of residual unbalance would cause obvious differences. From the results obtained (Figs. 6 through 9), it appears that the assumed value of unbalance may have been too small. At all other conditions of unbalance, any small difference between the true and assumed values of residual un-

balance would have been negligible since the applied unbalance was much larger than the residual unbalance.

Because the experimental values were consistently larger than the theoretical values in Figs. 6 through 9 and the possibility of having used too small a value of residual unbalance existed, it was decided to increase the value of residual unbalance in the analysis to the point where reasonable agreement could be obtained between theory and experiment. These comparisons are presented in Figs. 10 through 13. For these cases, it was found that an unbalance of 0.010 oz-in., which was four times as large as the assumed residual unbalance, was needed for reasonable agreement between theory and experiment. Since the amount

of unbalance needed for agreement was several times larger than that able to be detected by the balancing machine, the difference between theory and experiment for these cases is most likely not due to any small errors which might be present in the balancing machine.

Comparisons of theoretical and experimental data for rotor unbalances of 0.025, 0.037, and 0.050 oz-in. at the two bearing load conditions are presented in Figs. 14 through 19. For these unbalances, the comparison of experimental and theoretical values at the lower speeds (where the whirl amplitudes are small compared to bearing clearance) is fairly good. Differences are generally less than 0.00015 in. In the regions where the whirl amplitudes become larger than 40 to 50 percent of the bearing clearance, differences as large as 0.00035 in. occur. These differences can possibly be explained by the fact that the theory is only valid when the whirl amplitudes are small (eccentricity ratios less than 0.5) compared to bearing clearance. One exception to the above poor comparison is at the smallest bearing load condition where the comparison, regardless of the magnitude of experimental whirl amplitude, is fairly good for all three unbalances. Average differences for this bearing load condition were in the neighborhood of 0.0001 in., which is less than 10 percent of the total bearing clearance.

Conclusions

Several conclusions may be drawn from the experimental and theoretical comparisons reported here; they are, however, applicable only to the symmetrical rotor-bearing geometry investigated.

The first of these conclusions, is that the experimental values of whirl amplitude, regardless of the size of rotor unbalance, were generally larger than the theoretical values. One partial explanation for this discrepancy is the fact that the theory was not valid for the comparisons in the regions where whirl amplitudes approached bearing clearance. This fact was borne out by the results in that the comparison of theoretical and experimental values in the regions where whirl amplitudes were large compared to bearing clearance was only fair. Differences as large as 0.00035 in. were observed. One exception to this was for the smallest bearing load condition where the experimental

and theoretical comparisons were quite good regardless of the magnitude of experimental whirl amplitude. A second conclusion is that rotor speed and bearing load seemed to have a significant effect on the comparison of experimental and theoretical results. The closest comparisons were obtained at the lower rotor speeds and at the smallest of the two bearing loads.

Other than the areas where the whirl amplitudes were large compared to bearing clearance, it can be concluded that the overall agreement was reasonable. The actual differences between the theoretical and experimental values were small compared to bearing clearance and problems would only be encountered when amplitudes approached bearing clearance. Since the theory appears to generally under-predict rotor unbalance response, it is recommended that predictions made using the theory should be used only as approximations and safety factors be included in designs based upon these predictions.

Acknowledgment

The comparisons of experimental and theoretical rotor unbalance response presented in this paper were performed for the Fuels and Lubrication Division (AFAPL/SF), Air Force Aero Propulsion Laboratory, Wright-Patterson Air Force Base, under Contract AF 33(615)-69-C-1265.

References

- 1 Lund, J. W., "Rotor-Bearing Dynamics Design Technology—Part V: Computer Program Manual for Rotor Response and Stability," Technical Report AFAPL-TR-65-45, Part V, May 1965, Air Force Aero Propulsion Laboratory, Wright-Patterson Air Force Base, Ohio.
- 2 Prohl, M. A., "A General Method for Calculating Critical Speeds of Flexible Rotors," *Journal of Applied Mechanics*, Vol. 12, 1945, pp. 142–148.
- 3 Myklestad, N. O., *Journal of Aeronautical Sciences*, Vol. 11, 1944, p. 153.
- 4 Timoshenko, S., *Vibration Problems in Engineering*, D. Van Nostrand Company, 3rd Edition, 1955.
- 5 Lund, J. W. (Editor), "Rotor-Bearing Dynamics Design Technology—Part III: Design Handbook for Fluid Film Type Bearings," Technical Report AFAPL-TR-65-45, Part III, May 1965, Air Force Aero Propulsion Laboratory, Wright-Patterson Air Force Base, Ohio.